J2.1 RELATIONSHIP BETWEEN OPTICAL AND ICE CRYSTAL SHAPES IN MID-LATITUDE CIRRUS CLOUDS FROM POLAR NEPHELOMETER AND CPI

Jean – François Gayet[(1)], Guillaume Mioche[(1)], Valéry Shcherbakov[(1,2)], Christophe Gourbeyre[(1)], Reinhold Busen[(3)] and Andreas Minikin[(3)]

[1] Laboratoire de Météorologie Physique UMR 6016 CNRS / Université Blaise Pascal, France
[2] LaMP - Institut Universitaire de Technologie de Montluçon, France
[3] Deutsches Zentrum für Luft- und Raumfahrt, Institut für Physik der Atmosphäre, Oberpfaffenhofen, Germany.

1. INTRODUCTION

Optical phenomena like 22° halo and 46° halo were first explained by Mariotte (1717) as due to refraction of light (in the visible) by randomly oriented hexagonal ice crystals. Modelling studies of scattering phase functions show that these features are indication of highly regular pristine ice crystals (see among others Ping Yang et al., 2001). In this communication we describe two cases of in situ observations of cirrus clouds with both having mostly planar-plate ice crystals but with significant differences in optical properties in terms of 22° Halo occurrences. For one case, despite the fact that Polar Nephelometer data do not reveal any signature of 22° (and 46°) halos, preferential horizontal orientation of these plate-shaped crystals can explain systematic larger Lidar CALIOP retrieved extinctions compared to collocated in situ measurements (Mioche et al., 2010). For the second case, well-marked 22° halo features are observed along with prevalent planar-plate ice crystals. The interpretation of these results are discussed from a careful analysis of the ice particle morphologies and by using a theoretical model of light scattering (Shcherbakov et al., 2006). Implications for realistic modelling of scattering properties of cirrus clouds are given.

2. THE CIRCLE-2 EXPERIMENT AND AIRCRAFT INSTRUMENTATION

The CIRCLE-2 campaign (May 2007) involved the DLR Falcon aircraft equipped with microphysical and optical in situ probes, namely: the PMS FSSP-300 operated by the DLR, the Particle Cloud Imager (CPI), the Polar Nephelometer (PN) and the PMS 2D-C probes, operated by the Laboratoire de Météorologie Physique (LaMP). The combination of these three techniques provides a description of particles within a diameter range varying from a few micrometers (typically 3 μm) to about 2 mm. The method of data processing, the reliability of the instruments and the uncertainties of the derived microphysical and optical parameters have been described in detail by Gayet et al., (2009). Relative humidity was derived from measurements using a CR-2 frost point hygrometer. We will discuss in the next section relationships between optical properties and ice crystals morphologies from the interpretation of Polar Nephelometer and Cloud Particle Imager measurements obtained during the sampling of two cirrus clouds.

Corresponding author address: J-F Gayet, LaMP CNRS Université Blaise Pascal 63 171 Aubière, France; e-mail: gayet@opgc.univ-bpclermont.fr

3. RESULTS

3.1 *Cirrus properties with non-occurrence of 22° halo*

Representative example of cirrus properties with non-observed 22° halo feature (case A) is illustrated from observations carried out during a flight co-ordinated with CALIPSO overpass on 16 May 2007 in a thin frontal cirrus located West of France over ocean (Mioche et al., 2010). The sampling levels were located near the cirrus cloud top: 12000 m / - 59°C and 11600 m / - 55°C. Mean cirrus properties are displayed on Fig. 1. The left-upper panel shows the particle size distributions of the FSSP-300, 2D-C and CPI whereas the right-upper panel represents the scattering phase function measured by the Polar Nephelometer (filled circle symbols) and the theoretical phase function (cross symbols) calculated from the FSSP-300 size distribution assuming (spherical) ice crystals. The mean values of the parameters indicate ice particle concentration (1.4 cm^{-3}), concentration of particle with d > 100 μm (0.3 l-1), ice water content (2 mg/m^3), extinction coefficient (0.28 km^{-1}),

effective diameter (21 μm) and asymmetry parameter (0.788). The observed and the FSSP phase functions (see right-upper panel) show close agreement at the forward scattering angles (5°–50°). The CPI particle shape classification for ice crystals larger than 25 μm was performed by using the LaMP software (Lefèvre, 2007). The results were refined by operator supervision in order to reduce classification errors (Mioche et al., 2010). Pie-chart representation of the averaged particle shape classification (in surface percentages) on the left-bottom panel on Fig. 1 reveals 42% of plates, 10 % of needles and columns with 48% particles unclassified (irregular) as illustrated by examples of ice particle images (see right-bottom panel). Such plate ice crystals could be horizontally oriented and may therefore explain the poor extinction CALIPSO comparisons for that cirrus situation (Mioche et al., 2010). Despite the prevalence of regularly plate shaped ice crystals, surprisingly the Polar Nephelometer data do not reveal any signature of 22° halo with a featureless scattering phase function as highlighted on Fig. 1. Due to aerodynamical disturbances inside the shrouded probe inlets (Polar Nephelometer and CPI in this study) ice particles in the free air lose preferential orientation in the sampling section. A counterexample is discussed in the next section which describes cirrus properties also characteried by plate-shaped ice crystals but with related well-marked 22° halo peaks.

3.2 *Cirrus properties with 22° Halo occurrence*

This example (case B) concerns a cirrus cloud sampled over France on 16 May 2007 during the Falcon transit flight from Oberpfafenhoffen (Germany) to Brest (France). The flight level was -27°C / 7100 m. The results reveal occurrence of both well marked 22° halo and plate ice crystals on only rather small cloud parts (~ 4 km). Fig. 2 displays the corresponding mean cirrus cloud properties with a same representation as in Fig. 1. At forward angles (see panel b) the observed scattered energy (PN) is larger than the theoretical phase function (FSSP-300) indicating a significant contribution of particles larger than 20 μm (CPI data) on the scattering pattern. The mean values of the parameters indicate the ice particle concentration (1.9 cm^{-3}), concentration of particle with d > 100 μm (7.3 l-1'), ice water content (14 mg/m^3), extinction coefficient (0.49 km^{-1}), effective diameter (86 μm) and asymmetry parameter (0.795). Within this cloud sequence, the PN does clearly reveal 22° halo peak which occurs remarkably with the presence of ice crystals mostly pristine-plate shaped. Indeed, the Pie-chart (see left-bottom panel on Fig. 2) reveals 57% of plates, 16% of columns and needles, 12% of dendrite and side plane, with only 15% unclassified (irregular). Compared to the previous classification in Fig. 1, the smaller proportion of unclassified shapes is explained by larger ice crystals (89 μm versus 21 μm respectively) whereas plate crystals are found to dominate the ice particle populations for both examples with similar occurrences (57% versus 42% respectively).

4. DISCUSSION AND CONCLUSIONS

If the prevalence of plate ice crystals is a common feature of the two above examples, larger ice crystals are observed for the case B as exemplified on Fig. 3.a which displays the halo ratio versus the mean volume diameter (MVD) derived from the CPI size distributions (case B data, see Fig. 2). Since the Polar Nephelometer measures the scattered energy at scattering angles of 22° and 18.5°, the ratio of these energy values provides a quantitative criteria (called hereafter halo ratio) which characterizes the 22° halo feature (Auriol et al., 2001). High halo ratio (> 1.0) reveals sharp peaks with well-pronounced 22° halo whereas smoothed peaks and/or smoothed scattering phase functions with no 22° halo are characterized by smaller halo ratio (< 1). On Fig. 3.a well marked 22° halo peaks (halo ratio > 1) are found for *MVD* ranged between 50 to 250 μm. The superimposed data (case A with no halo) are distributed over a smaller *MVD* range (< 130 μm) and with dimension larger than 20 μm. This value appears to delineate the lower limit of ice crystal size responsible (at visible wavelengths) for halo formation following earlier studies (Shcherbakov et al., 2006). Therefore, the reported ice crystal sizes do not appear critical for the halo/no-halo interpretation.

A careful examination of the CPI images reveals that most of the recorded ice crystal plates on Fig. 2.d present a quite regular shape with a perfectly transparent internal structure. Indeed, refraction through the 60° prisms of such plates will produce very sharp scattering peak near 22°. If objective observation of CPI images on Fig. 1.d also highlights quite regular plate shape, on the contrary, most of them present an imperfect internal structure with well recognizable heterogeneity. This proves the consistency of our observations that halo feature is evidenced only

with the presence of perfect plate ice crystals (or pristine crystals strictly speaking). This also means that the Polar Nephelometer data contains signature of pristine ice crystals. Defaults in crystal geometry, roughness of the ice surface or internal heterogeneity do hamper the formation of halo. The model from Shcherbakov et al. (2006) was used to compute the angular scattering patterns for measured crystal shape and size and by considering both roughness and internal structure. In this model the surface roughness assumes the Weibull statistics and the air bubbles density is hypothesized to represent the crystal internal heterogeneity. Ice plates and columns were modelled by quasi-hexagonal prisms with the aspect ratio of 0.2 and 2, respectively. To smooth the 46° halo peak, the hexagonal planes were divided into a number of facets. And, the vertices of the facets were randomly shifted along the "C" axis of the crystal. The shift was within 10% of the crystal length. The particle shape classification was considered in terms of particle surface (see Pie-charts). The fitting results are shown by the red points on figures. The smoothed scattering pattern (Fig. 1.b) was obtained for the deeply rough surface of crystals with heavy load of inclusions. The scattering pattern with 22° halo (Fig. 2.b) was computed for the slightly rough surface of crystals that have no inclusions.

The azimuthal halo pattern of the scattering behaviour enhances significantly the asymmetry parameter as exemplified on Fig. 3.b. The larger *g* is (from 0.780 to 0.805) more pronounced is the 22° halo peak (0.74 < halo ratio < 1.50), simply because the energy is more scattered in the forward direction. Highly regular or pristine ice crystals are expected to result from extremely regular crystal growth. Figs. 3.c & d display the scatter plots of the halo ratio versus relative humidity (over ice) and vertical airspeed respectively. Fig. 3.c reveals that the 22° halo peaks are distributed mostly around 100% of RHi and confirm the findings from Heymsfield (1986) that low ice supersaturations are known to favour regular and slow crystal growth. This feature should be found in low updraft velocities but results on Fig. 3.d rather show that halo ratios are more pronounced for increasing updrafts. The analysis of our results shows that only a few cloud portions characterized by small horizontal scales (ranged from 1000 m to 4000 m) present halo signature and therefore pristine ice crystals. According to the large data set obtained in mid-latitude cirrus clouds during INCA, these areas represent only 3% of the sampled cirrus (Gayet et al., 2004). This means that simple pristine crystals are uncommon but rather complex manifestations (shape defaults, roughness, inclusions, …) of these are prevailing. Following the findings of Baran (2004) modelling of ice crystal ensemble rather than single crystals should better represent cirrus single-scattering properties. Our large data set in cirrus (at mid-latitudes) clearly evidence that phase functions are smooth and featureless and best represent scattering properties from cirrus.

Acknowledgements. This work was funded by the Centre National d'Etudes Spatiales (CNES) and by a grant from the CNRS/INSU. The contribution of DLR as well as large part of Falcon flight hours was funded in the framework of the DLR PAZI-2 project. We thank the members of DLR (Deutsches Zentrum für Luft- und Raumfahrt) and SAFIRE (Service des Avions Français Instrumentés pour la Recherche en Environnement) who organized the experiment management and aircraft operations. We acknowledge A. Schwarzenboeck and J-F Fournol (LaMP), B. Weinzierl and H. Rüba (DLR) for their active participation in the experiment.

References

Auriol F., J-F Gayet, G. Febvre, O. Jourdan, L. Labonnote and G. Brogniez ,2001:, In situ observations of cirrus cloud scattering phase function with 22° and 46° halos : Cloud field study on 19 February 1998. *J. Atmos. Sci*., **58**, 3376-3390.

Baran, A.J., 2004: On the scattering and absorption properties of cirrus cloud, *J. Quant. Spect. & Rad. Tran.*, **89**, 17–36.

Gayet J-F, J. Ovarlez, V. Shcherbakov, J. Ström, U. Schumann, A. Minikin, F. Auriol, A. Petzold, and M. Monier, 2004: Cirrus cloud microphysical and optical properties at southern and northern midlatitudes during the INCA experiment. *J. Geophys. Res.,* **109**, D20206, doi:10.1029/2004JD004803.

Gayet J-F, G. Mioche, A. Dörnbrack, A. Ehrlich, A. Lampert and M. Wendisch, 2009: Microphysical and optical properties of Arctic mixed-phase clouds.The 9 April 2007 case study. *Atmos. Chem. Phys.*, **9**, 1-15.

Heymsfield, A. J., 1986: Ice particles observed in a cirriform cloud at -83°C and implications for polar stratospheric clouds, *J. Atmos. Sci.,* **43,** 851–855.

Lefèvre, R., 2007 : Physique de la mesure de la sonde CPI pour la mesure des propriétés des cristaux de glace. Application aux observations

réalisées durant la campagne ASTAR 2004, Université Blaise Pascal, Aubière, France, 186 pp.
Mariotte, E., 1717 : Oeuvres de Mr. Mariotte. *Traité des couleurs,* Vol. **1**, P. Vander, Ed., 272–281.
Mioche G., D. Josset, J-F Gayet, J. Pelon, A. Garnier, A. Minikin and A. Schwarzenboeck, 2010: Validation of the CALIPSO/CALIOP extinction coefficients from in situ observations in mid-latitude cirrus clouds during CIRCLE-2 experiment. *J. Geophys. Res.*, in press.
Shcherbakov V., J.-F. Gayet, B. Baker and P. Lawson, 2006: Light scattering by single natural ice crystals. *J. Atmos Sci*., **63**, 1513-1525, DOI 10.1175/JAS3690.1.
Yang, P., B. C. Gao, B. A. Baum, W. J. Wiscombe, Y. X. Hu, S. L. Nasiri, P. F. Soulen, A. J. Heymsfield, G. M. McFarquhar, and L. M. Miloshevisch, 2001: Sensitivity of cirrus bidirectional reflectance to vertical inhomogeneity of ice crystal habits and size distributions for Moderate-Resolution Imaging Spectroradiometer (MODIS) bands, *J. Geophys. Res.*, ***106***, 17,267-17, 291.

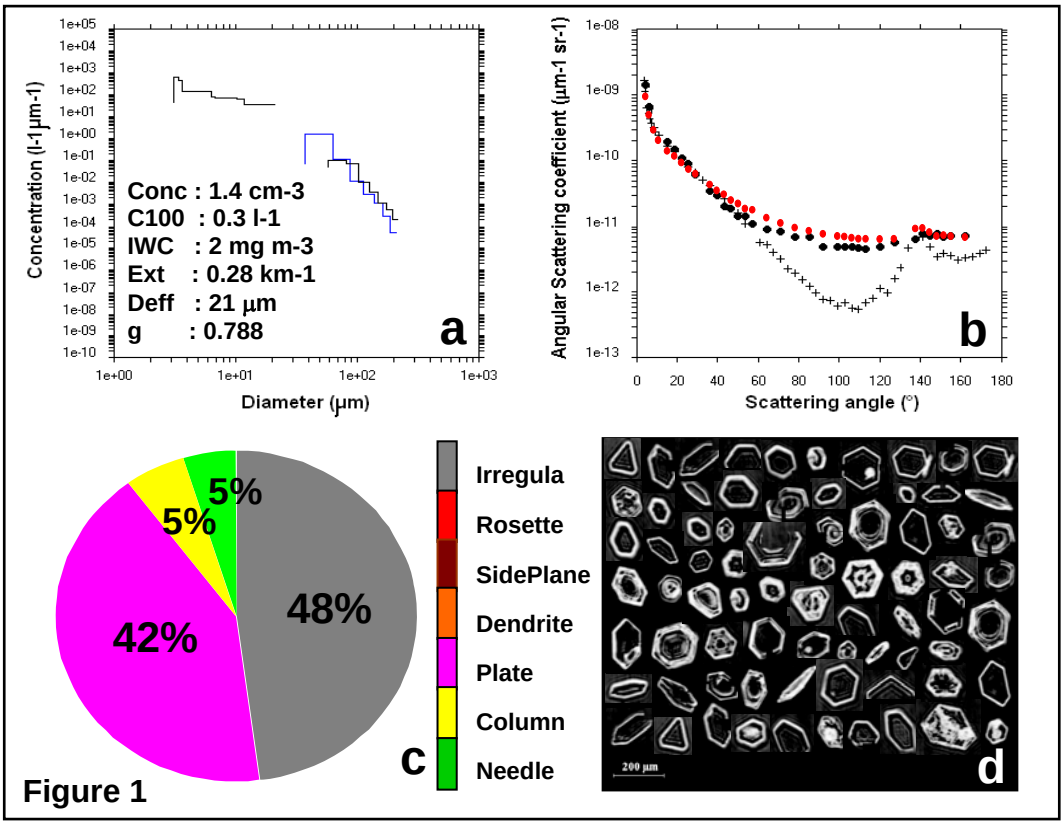

Figure 1

Figure 1. Mean properties of cirrus cloud sampled between -56°C and – 55°C (case A). Panels (a) : FSSP-300, 2D-C and CPI particle size distributions ; (b) : Scattering phase function measured by the Polar Nephelometer (filled black circle symbols), phase function (cross symbols) calculated from the FSSP-300 size distribution assuming (spherical) ice crystals and modelled phase function (red circle symbols); (c) : Pie-chart representation of the averaged particle shape classification ; (d) : Illustrative examples of ice particle images from the CPI instrument. Averaged values of microphysical and optical parameters are indicated on the (a) panels.

Figure 2 (see below). Same as Fig. 1. Cirrus sampled at -27°C (case B).

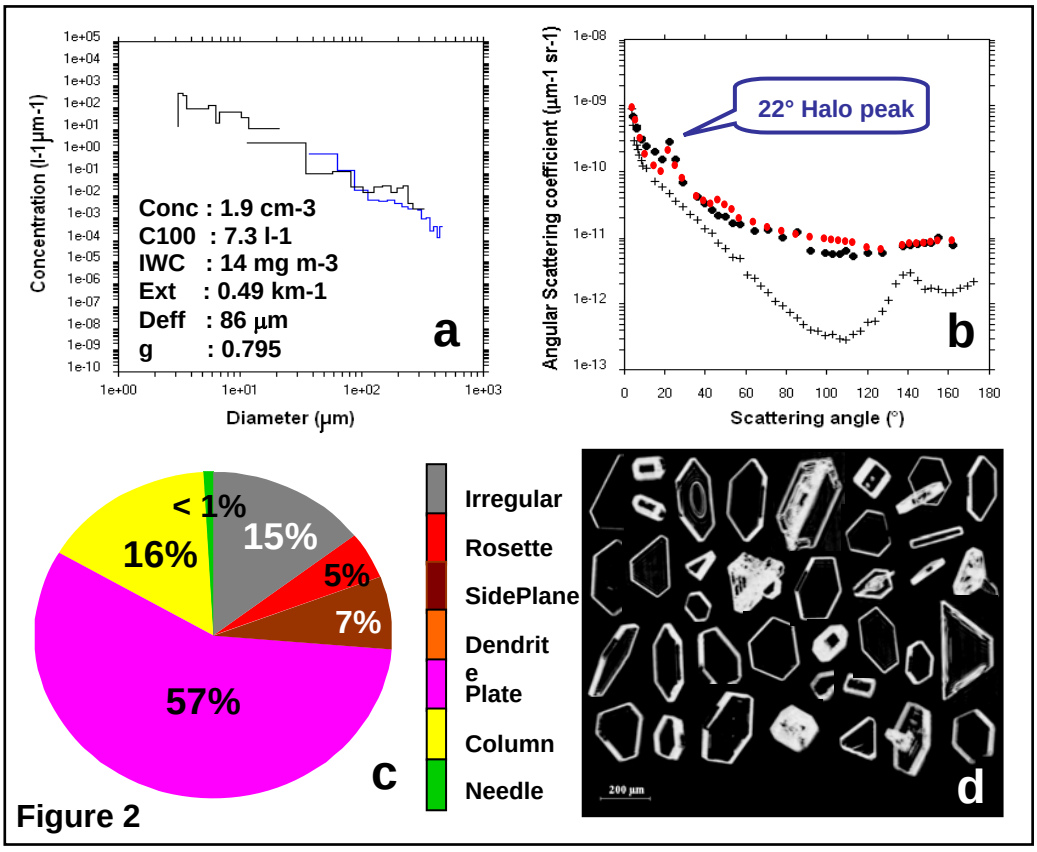

Figure 2

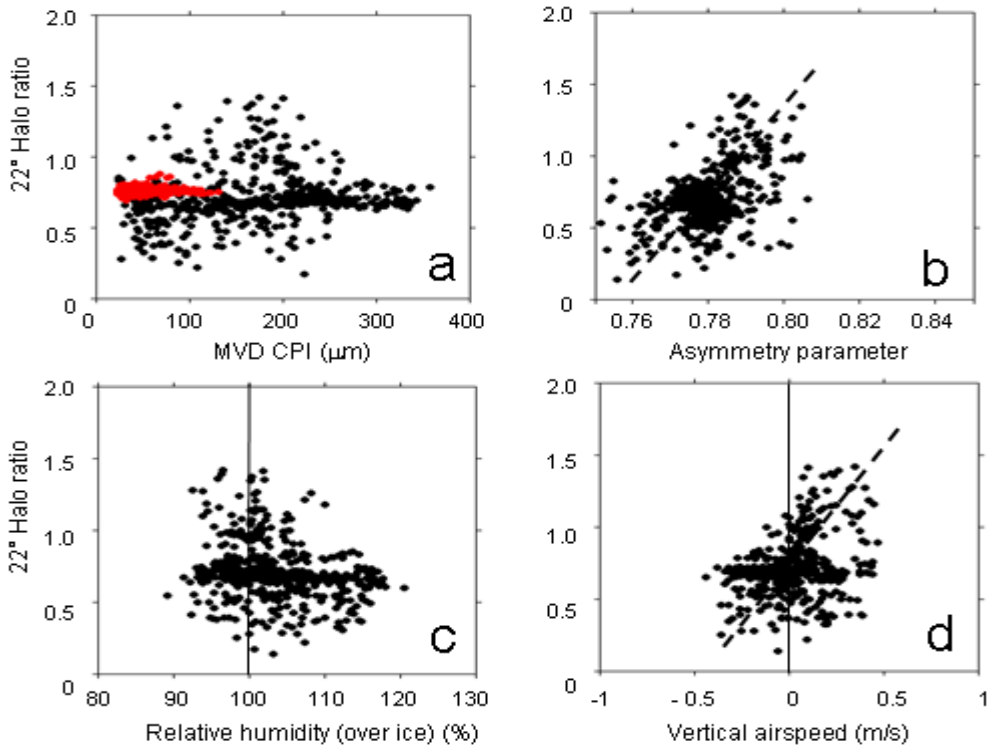

Figure 3. Scatter plots of the halo ratio versus : (a) the mean volume diameter from CPI (MVD), (b) the asymmetry parameter, (c) the relative humidity over ice and (d) the vertical airspeed. The data relate cirrus with 22° Halo occurrence (case B, see Fig. 2 right panel). The red points on Fig. 3.a concern the cirrus with no 22° Halo (case A).